

In Situ Thickness Determination of Adsorbed Layers of Poly(2-Vinylpyridine)–Polystyrene Diblock Copolymers by Ellipsometry

Ryan Toomey,[†] Jimmy Mays,[‡] and Matthew Tirrell^{*,†}

Materials Research Laboratory, University of California at Santa Barbara, Santa Barbara, California 93106, and Department of Chemistry, University of Tennessee, Knoxville, Tennessee 37996

Received July 10, 2003; Revised Manuscript Received November 14, 2003

ABSTRACT: To gain more insight into the process of formation of adsorbed layers of diblock copolymers, ellipsometry was used to monitor in situ the thickness and adsorbed amount of a series of polystyrene-*b*-poly(2-vinylpyridine) diblock copolymers adsorbed on silicon from toluene. First, it is demonstrated that ellipsometry can be sensitive to both the zeroth (Γ_0) and first (Γ_1) moments of the interfacial density profiles of the PS/PVP layers, providing sufficient information to measure the thickness $2\Gamma_1/\Gamma_0$ at each stage of the adsorption process. Second, it is found that in the early stages of layer formation, at the point where adsorbed chains are forced to laterally overlap, the thickness of the PS/PVP layers is equal to approximately $2.2R_g$. As the adsorbed amount surpasses approximately twice this surface density, the thickness grows as the layer becomes progressively more crowded. In this growth regime, the dependence of the thickness on the adsorbed amount makes a transition to a one-third power-law at the highest adsorbed amounts.

Introduction

One of the most versatile methods to create soft, tailored interfaces is through the adsorption of amphiphilic block copolymers.¹ The principal advantage in using block copolymers is the ability to self-assemble into layers with a specific structure depending on the architecture of the copolymer. For instance, the adsorption of A–B type diblock copolymers from a selective solvent produces a brush structure where one block preferentially tethers the other to the surface.^{2,3} While much experimental attention has focused on the relationship between the structure of the adsorbed layer and molecular details of the block copolymer, much less is understood about the adsorption process itself. Part of this ambiguity is rooted in the large number of potential configurations a macromolecule may adopt when adsorbing to a surface. A common approach to studying adsorbed layers has been to alter some aspect of the block copolymer, such as molecular weight or the asymmetry ratio, and then to characterize the adsorbed layer using neutron reflection^{4–7} or the surface forces apparatus.^{7–11} However, few methods give real-time, in situ information on the assembly process.

The process of layer formation is currently understood as consisting of an initial fast regime, during which chains diffuse from solution to occupy an empty surface, followed by a slower buildup of surface density by the penetration of chains through the developing adsorbed layer along with molecular rearrangement of the layer.¹² Various experimental reports in which the kinetics of adsorption were measured are in qualitative agreement with this kinetic picture;^{13–17} however, most of these studies report only the time dependence of the adsorbed amount and do not provide concurrent information on the structure of the adsorbing layer. An attempt has

been made to study the adsorption kinetics of polystyrene–poly(2-vinylpyridine) diblock copolymers with the SFA;¹⁸ however, the SFA is slow and not well suited to monitor adsorption kinetics. Information at short adsorption times cannot be gathered.

A more detailed understanding of the adsorption process can be established by measuring in situ both the adsorbed amount and the thickness of the layer at each stage of the adsorption process. This dual measurement sheds light on how polymer chains initially populate the surface as well as how the structure of the layer evolves as the layer becomes increasingly more populated. A fundamental issue in the adsorption of block copolymers is whether the adsorption kinetics and layer structure can be predicted from thermodynamic arguments or if the structure is dominated by kinetic issues. For instance, how a chain initially adsorbs to the surface may be a function of the particular manner in which it arrives at the surface, but then it must rearrange to adopt its thermodynamically preferred structure. The speed of these rearrangements will impact both the structure of the layer and the nature of the potential barrier that a free chain must overcome in order to adsorb.

Therefore a characterization technique is desired that can provide both the thickness and adsorbed amount quickly and simultaneously. Ellipsometry, which is based on the interference between reflected s- and p-polarized light, detects both the relative amplitude and phase change of the reflected waves at a single angle of incidence.¹⁹ For thin adsorbed layers that are much less than the wavelength λ of light and that are sufficiently dilute (where the refractive index of the layer approaches the refractive index of the solvent), these two quantities measured by the ellipsometer are sensitive to only the zeroth Γ_0 and first moments Γ_1 of the interfacial index profile.^{20,21} Higher order moments of the index profile do not contribute to the ellipsometry measurement. Therefore, in this limit, a measurement at a single angle provides enough information to resolve

* To whom correspondence should be addressed. E-mail: tirrell@engineering.ucsb.edu.

[†] University of California at Santa Barbara.

[‡] University of Tennessee.

Table 1. Properties of PS–PVP Diblock Copolymers

Sample	M_n PS block, g/mol	M_n PVP block, g/mol	M_w/M_n
PS–PVP: 25K/4K	24 900	3 600	1.10
PS–PVP: 40K/10K	40 100	9 900	1.06
PS–PVP: 100K/12K	99 900	12 100	1.04
PS–PVP: 255K/24K	255 100	23 800	1.06

both the adsorbed amount defined as $\Gamma(\text{mass/area}) = \Gamma_0(dn/dc)^{-1}$, where dn/dc is the refractive index increment of the polymer, and the thickness of the adsorbed layer is defined as $2\Gamma/\Gamma_0$.

In this paper, it is demonstrated that ellipsometry can monitor in situ both the adsorbed amount and thickness $2\Gamma/\Gamma_0$ of a series of polystyrene-*b*-poly(vinyl pyridine) diblock copolymers adsorbed from toluene to the surface of silicon. The poly(2-vinylpyridine) block provides the driving force for adsorption, effectively tethering to the surface the nonadsorbing polystyrene block. The results show that above approximately twice the overlap density the layer thickness starts to grow with a power law that approaches a one-third dependence on the adsorbed amount. The study shows that, under these conditions, adsorbing layers of PS/PVP have the capacity to rearrange quickly enough such that the thickness grows according to thermodynamic predictions, indicative that the adsorbed layer is tending toward its equilibrium configuration at each stage in the adsorption process. Thus, while extremely large adsorption barriers may prevent a system from realizing its equilibrium adsorbed amount, the structure developed during the adsorption process is not necessarily hindered by kinetic barriers.

Experimental Section

Materials. Diblock copolymers of polystyrene and poly(2-vinylpyridine) were synthesized by anionic polymerization. Both monomers were obtained from Aldrich. Styrene was purified on a high vacuum line by sequential exposure to and distillation from freshly ground calcium hydride and dibutylmagnesium. 2-Vinylpyridine was purified by exposure to and distillation from calcium hydride, sodium mirrors, and triethylaluminum. The purified monomers were distilled into calibrated ampules equipped with breakseals and stored in a freezer until used. *n*-Butyllithium (Aldrich) was diluted in vacuo with purified hexanes and used as an initiator. Tetrahydrofuran (THF, Fisher) was used as solvent after purification with calcium hydride, sodium dispersion, and sodium naphthalenide on the vacuum line. Polymerization involved distillation of THF into the reactor followed by heat sealing from the vacuum line and introduction of *n*-BuLi into the reactor. Polymerization of styrene was accomplished by breaking the glass seal, followed by distillation of this monomer into the stirred reactor at -78°C . After 1 h, the seal to the 2-vinylpyridine was broken and this monomer was allowed to slowly distill into the reactor and 30 min was allowed for polymerization of the second block, followed by termination with degassed methanol. The block copolymers were precipitated into hexanes and characterized by proton NMR and size exclusion chromatography (SEC). THF containing 1% triethylamine (TEA) was used as the mobile phase, and molecular weights and polydispersities were calculated by using a polystyrene calibration curve. Tertiary amines are known to suppress adsorption of PVP onto SEC columns and it was confirmed that the addition of a small amount of TEA had no effect on the elution behavior of PS standards. SEC with polystyrene standards should give reliable molecular weights due to the low PVP content in the diblocks, as well as the structural similarity between PS and PVP. Molecular characteristics are summarized in Table 1.

Instrumentation. The adsorption experiments were conducted on a variable-angle Beaglehole picometer ellipsometer, which uses a He–Ne laser light source ($\lambda = 632.8\text{ nm}$), has an angular resolution of 0.01° , and is based on the phase modulation technique of Jasperson and Schnatterley.²² The ellipsometer directly measures the real and imaginary components of the ellipsometric ratio

$$\rho = \frac{r_p}{r_s} = \tan \Psi e^{i\Delta} \quad (1)$$

where $\text{Re}(\rho) = \tan \Psi \cos \Delta$ and $\text{Im}(\rho) = \tan \Psi \sin \Delta$. r_p and r_s are the complex overall reflection coefficients of the p- and s-polarizations, respectively. The angles Ψ and Δ correspond to the ratio of attenuation of the p- and s-polarizations and the phase change between the p- and s-polarizations, respectively.

Experimental Procedure. For the adsorption experiments, a freshly cleaned silicon wafer is placed in the center of specially built cylindrical glass cell with a total volume of 17 mL. The average thickness of the silicon oxide layer ($n = 1.46$) is on the order of 15 \AA . The refractive index n of silicon is $3.88 - i0.019$. Fresh toluene ($n = 1.4926$) is added to the cell, and the angle of incidence is adjusted until $\Delta = 90^\circ$, which defines the Brewster angle. This angle was usually within 0.25° of the expected angle of 68.95° for the toluene/silicon interface. At this incidence, $\text{Re}(\rho) = 0$ and $\text{Im}(\rho)$ has a small, positive value typically around 5×10^{-3} . As discussed in the Appendix, $\text{Im}(\rho)$ should be zero at the Brewster angle between two perfect dielectric media (or media having no imaginary part to their refractive index). The experimental source of the nonzero value of $\text{Im}(\rho)$ comes from three principal contributions: a small imaginary component to the refractive index of silicon, the presence of the 15-\AA oxide layer on the silicon, and slight birefringence in the glass cell. At these low values of $\text{Im}(\rho)$, however, all contributions to $\text{Im}(\rho)$ are additive. This reading serves as a baseline and only the change in $\text{Im}(\rho)$ upon adsorption is important.

The readings in both $\text{Re}(\rho)$ and $\text{Im}(\rho)$ were then checked over the course of 15 min to verify consistency. The noise in the readings was usually (2×10^{-5} in both $\text{Im}(\rho)$ and $\text{Re}(\rho)$). If the readings did not change by more than 3×10^{-5} , approximately 1–10 mL of the stock PS–PVP solution was added to the solution cell to make a final concentration of $30\text{ }\mu\text{g/mL}$. At this dilute polymer concentration, the copolymers are molecularly dissolved and not in an aggregated, micellar state.¹³ The changes in $\text{Re}(\rho)$ and $\text{Im}(\rho)$ were measured every 0.5 s for 5–10 h of adsorption time.

Data Analysis. The changes in $\text{Re}(\rho)$ and $\text{Im}(\rho)$ upon adsorption are directly proportional to the first Γ_1 and zeroth moments Γ_0 of the refractive index profile of the adsorbed layer:

$$\text{Re}(\rho) = (2\pi)2n_{\text{solvent}}\left(\frac{2\Gamma_1}{\lambda^2}\right) \quad (2)$$

$$\text{Im}(\rho) - \text{Im}(\rho)_{\text{baseline}} = (2\pi)\frac{\sqrt{n_{\text{substrate}}^2 + n_{\text{solvent}}^2}}{n_{\text{solvent}}}\left(\frac{\Gamma_0}{\lambda}\right) \quad (3)$$

Both eqs 2 and 3 are derived in the Appendix. $n_{\text{substrate}}$ and n_{solvent} refer to the refractive indices of silicon and toluene, respectively. Equations 2 and 3 represent mean-field averages of the lateral distribution of the bound polymer layer. This condition breaks down only at sufficiently low surface coverages, where the distance between bound polymer chains is much longer than the wavelength of the incident light source. The small imaginary contribution to the refractive index of silicon was and can be safely ignored in eq 3. The adsorbed amount Γ (mass/area) is readily evaluated from Γ_0 by

$$\Gamma(\text{mass/area}) = \Gamma_0\left(\frac{dn}{dc}\right)^{-1} \quad (4)$$

where dn/dc is the refractive index increment of the polymer, 0.102 mL/g. As PS and PVP are nearly isorefractive, the refractive index increment of the copolymer is insignificantly influenced by its composition. Finally, the thickness $2\Gamma_1/\Gamma_0$ can be defined

$$\frac{\text{Re}(\rho)}{\text{Im}(\rho) - \text{Im}(\rho)_{\text{baseline}}} = \left(\frac{2\pi}{\lambda}\right) \frac{n_{\text{solvent}}^2}{\sqrt{n_{\text{solvent}}^2 + n_{\text{substrate}}^2}} \left(2\frac{\Gamma_1}{\Gamma_0}\right) \quad (5)$$

The ratio $2\Gamma_1/\Gamma_0$ represents the average thickness of the density profile of the adsorbed polymer layer. For a film with a uniform dielectric profile, $2\Gamma_1/\Gamma_0$ is exactly the overall thickness; for monotonically decreasing dielectric profiles, $2\Gamma_1/\Gamma_0$ is less than the overall thickness. For highly solvated layers, ellipsometry cannot yield any more information other than the zeroth and first moments of the density profile.

Figure 1 shows the applicability of eq 5. The ellipsometric ratio ρ was calculated for series of hypothetical PS-PVP layers adsorbed in toluene on silicon surfaces with three types of refractive index profiles for the adsorbed layer: step, parabolic, and Gaussian. The Gaussian form was used to simulate a mushroom-type regime. For instance, in the case of the parabolic profile, the following refractive index profile was used

$$n(z) = \Delta n_0 \left(1 - \left(\frac{z}{L}\right)^2\right) + n_2 \quad (6)$$

The profile was approximated as a series of homogeneous slabs of 10 Å width and an iterative method employing the full equation of ellipsometry (as outlined in Azzam and Bashara¹⁹) was used to determine the ellipsometric ratio ρ as a function of $2\Gamma_1/\Gamma_0$. The refractive index of the solvent 1.4926, the refractive index of the substrate 3.88 – ± 0.019 , and $\Delta n_0 = 0.05$.

Figure 1 shows the numerically tabulated values $\text{Re}(\rho)/\text{Im}(\rho)$ using the full equation of ellipsometry as well as the analytical approximation of eq 5. As seen, the upper limit of applicability is approximately 700 Å, where higher moments start to contribute to ρ . More generally, the following restrictions must be met in order for eq 5 to be applicable

$$\Delta n_{\text{film}} \ll n_{\text{solvent}} \quad (7)$$

$$|\Delta n_{\text{film}}| \ll |n_{\text{substrate}} - n_{\text{solvent}}| \quad (8)$$

$$\Gamma_1 < \left(\frac{\lambda}{2\pi}\right)^2 \quad (9)$$

Results and Discussion

Response of $\text{Im}(\rho)$ and $\text{Re}(\rho)$ to the Adsorption of PS/PVP. Figure 2 shows the raw ellipsometric data expressed as imaginary and real parts of the ellipsometric ratio ρ for the adsorption of the 100K/12K and 255K/24K PS/PVP samples. Both components show a fast rise in the first 1000 s followed by a much slower increase. Since $\text{Im}(\rho)$ is directly proportional to the adsorbed amount, it can be readily inferred from this data set that the 100K/12k sample adsorbs more quickly than the 255K/24K sample. Furthermore, the transition from the fast to slow growth regimes occurs at a higher value of $\text{Im}(\rho)$ in the 100K/12K sample than in the 255K/24K sample, which can be understood with respect to the relative sizes of the two samples. The larger molecular weight of the 225K/24K sample translates to a slower adsorption rate and lower crossover surface coverage, both of which are readily apparent in the $\text{Im}(\rho)$ curves shown in Figure 2.

In contrast to $\text{Im}(\rho)$, however, the real part of the ellipsometric ratio $\text{Re}(\rho)$ displays the opposite trend with respect to molecular weight. Since $\text{Re}(\rho)$ is proportional to the first moment of the dielectric profile, or the square

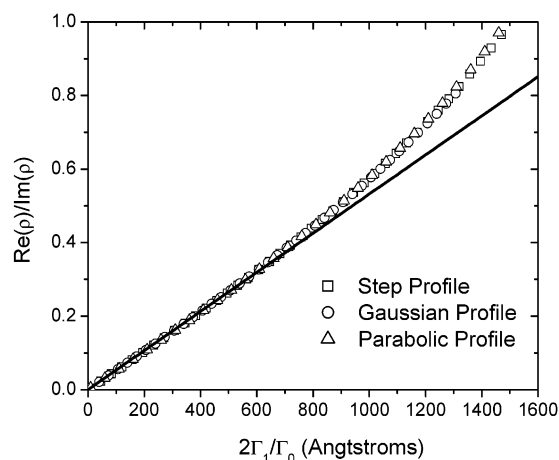


Figure 1. $\text{Re}(\rho)/\text{Im}(\rho)$ versus $2\Gamma_1/\Gamma_0$ for a step, Gaussian, and parabolic profile. The refractive index of the solvent 1.4926, the refractive index of the substrate $n_1 = 3.88$, and $\Delta n_0 = 0.05$. The straight line corresponds to the analytical simplification of eq 5.

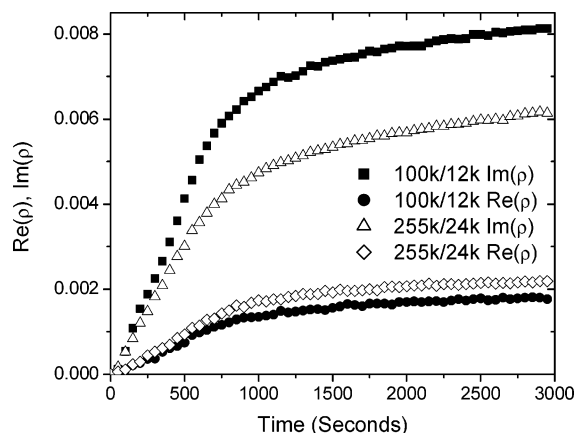


Figure 2. Response of $\text{Re}(\rho)$ and $\text{Im}(\rho)$ to the adsorption of the 100K/12K and the 255K/24K samples as a function of time.

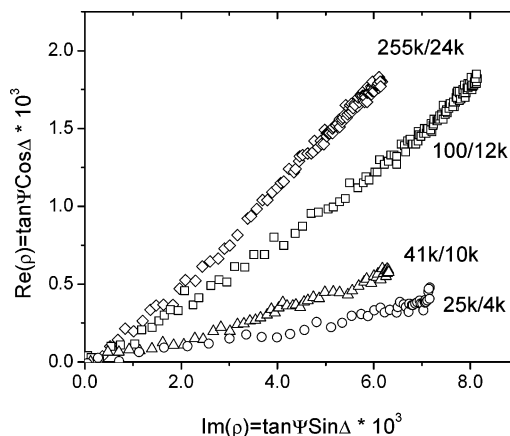


Figure 3. Plot of the $\text{Im}(\rho)$, $\text{Re}(\rho)$ trajectories for the four PS/PVP samples.

of thickness, it gives information concerning the degree to which the adsorbed layer extends from the surface. The 255K/24K copolymer has more than twice as many segments as the 100K/12K sample; therefore, it will produce a thicker adsorbed layer than the 100K/12K sample. In general, the larger the PS block, the larger the signal generated in $\text{Re}(\rho)$. Figure 3 better exemplifies this trend by showing the $\text{Re}(\rho)$, $\text{Im}(\rho)$ trajectories for all four molecular weights. At values of $\text{Im}(\rho)$ less

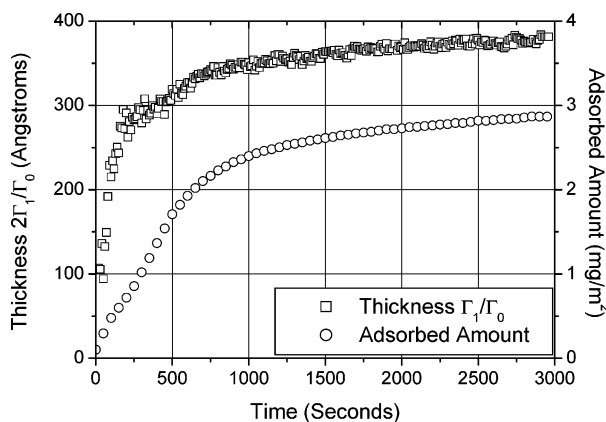


Figure 4. Time evolution of both the adsorbed amount and the thickness $2\Gamma_1/\Gamma_0$ for PS/PVP 100K/12K sample adsorbed from toluene to silicon.

than approximately 10^{-3} (corresponding to $\Gamma = 0.37 \text{ mg/m}^2$) there is significant scatter in the $\text{Re}(\rho)$ data, as manifested in the overlap of $\text{Re}(\rho)$ between the different molecular weights. Since $\text{Re}(\rho)$ scales as the square of thickness, it is much less sensitive than $\text{Im}(\rho)$ to the presence of the adsorbed layer. Therefore, at sufficiently low surface coverages, $\text{Re}(\rho)$ is not resolvable, and in this limit the layer thickness cannot be determined. At higher values of $\text{Im}(\rho)$, however, more contrast is generated, and the four samples start to follow different trajectories. The larger molecular weights display larger values of $\text{Re}(\rho)$ and at the same $\text{Im}(\rho)$ due their larger extension from the surface.

Analysis of Adsorption Kinetics. The $\text{Im}(\rho)$, $\text{Re}(\rho)$ trajectories for each PS/PVP sample can be recast as an adsorbed amount and a thickness $H_{\text{elli}} = 2\Gamma_1/\Gamma_0$, according to eqs 2–4, respectively. As an example, Figure 4 shows the change in both the adsorbed amount and thickness for the 100K/12K sample. It has been previously observed that adsorption of neutral diblock copolymers in a selective solvent proceeds via a two-stage process.^{13,16} At early times, layer growth is limited by the transport of individual chains to the surface, which is a function of their diffusion coefficient D . In the absence of any convection, it is expected that the adsorbed amount should increase with the square root of time¹²

$$\Gamma(t) = 2c_{\text{polymer}}\sqrt{\frac{Dt}{\pi}} \quad (10)$$

where c_{polymer} is the polymer concentration.

This rate law should be valid assuming the following two statements: (1) the absence of interactions between adsorbing chains and previously adsorbed chains and (2) every chain that approaches the surface sticks to it. Experimentally, however, it was found that even at the earliest times, the adsorption rate of all samples is approximately an order of magnitude slower than the rate predicted by eq 9. For instance, Figure 5 compares the adsorption of the 100K/12K sample to the prediction of eq 10 using its diffusion coefficient of $4.1 \times 10^{-7} \text{ cm}^2/\text{s}$. Not only is the experimental rate slower than that predicted by the diffusion coefficient, but the experimental initial rate also displays a stronger power dependence on time than anticipated from eq 10, which is closer to 0.8 than 0.5. This observation is probably the manifestation of significant interactions between incoming chains and preexisting adsorbed chains oc-

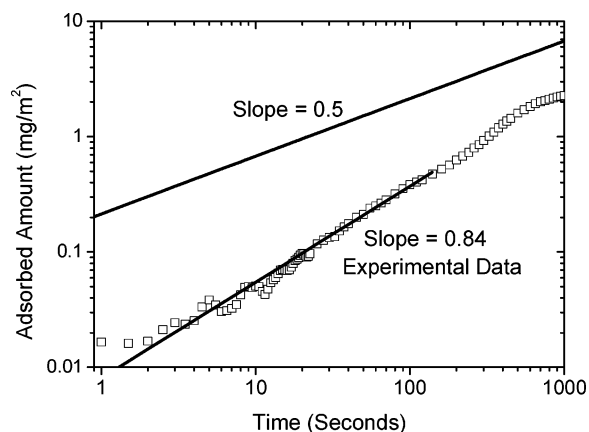


Figure 5. Comparison of the initial adsorption kinetics of the PS/PVP 100K/12K sample with the theoretical prediction of eq 10 for diffusion-limited adsorption.

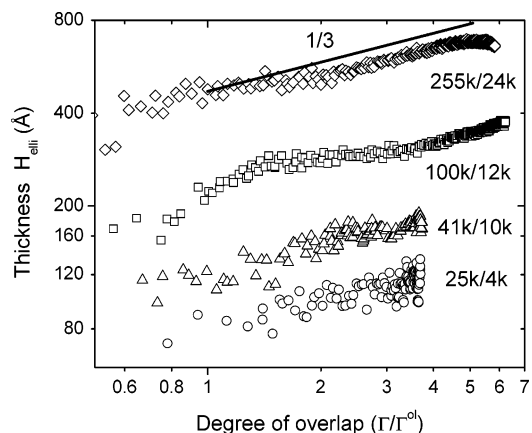


Figure 6. Log-log plot of the thickness $2\Gamma_1/\Gamma_0$ vs the average degree of overlap. The line represents the one-third scaling regime expected for brushes in a good solvent environment.

curing even at very low adsorbed amounts. In terms of thickness data, the first measurable thickness occurs at approximately 100 Å , corresponding to an adsorbed amount of 0.25 mg/m^2 . As the adsorbed amount increases to 0.75 mg/m^2 , the thickness triples to almost 300 Å , which occurs in the first 200 s of adsorption, where the thickness remains relatively constant until the adsorbed amount surpasses 1.75 mg/m^2 . After this stage, the thickness again increases with increasing adsorbed amount.

A more straightforward analysis can be conducted if H_{elli} is plotted against the degree of overlap Γ/Γ^{o1} for the four PS–PVP samples, as shown in Figure 6. A value of $\Gamma/\Gamma^{o1} = 1$ corresponds to the surface coverage where neighboring chains, on average, begin to overlap. The overlap concentration is defined as

$$\Gamma^{o1} = m_0 N / \pi < abv > R_{\text{PS}}^2 \quad (11)$$

where m_0 is the weight of a monomer, N is the degree of polymerization, and R_{PS} represents the radius of gyration for the PS in dilute toluene solutions. The data for R_{PS} in toluene has been reported by Higo et al.:²³

$$R_{\text{PS}} = aN_{\text{PS}}^\nu \quad (12)$$

where $a = 1.86 \text{ Å}$ and $\nu = 0.595$. From Figure 6, it is seen that at low degrees of overlap, $\Gamma/\Gamma^{o1} < 1$, the thickness increases somewhat until it reaches a pseudo-

plateau around $\Gamma/\Gamma^0 \approx 1$. This is especially prevalent in the two larger molecular weights, 255K/24K and 100K/12K. The data were limited to values of $\Gamma/\Gamma^0 > 0.5$, as there is too much scatter at lower surface coverages to reliably determine the thickness. The most plausible explanation for the increase in layer height at early times stems from a weak interaction between the polystyrene buoy blocks and the surface. As the chains initially impinge the surface, they adapt a slightly flattened configuration but quickly rearrange such that the PVP block is strongly adsorbed and the PS block is only weakly adsorbed, if adsorbed at all. Previous experiments have shown that the interaction between PS and silicon dioxide in toluene is not sufficient to overcome its resulting loss in translational entropy upon adsorption and therefore PS alone does not adsorb.¹⁶

In the range of weak overlap ($1 < \Gamma/\Gamma^0 < 2$), the thicknesses are relatively independent of the adsorbed amount. In this pseudoplateau region, the measured thicknesses H_{elli} are considerably larger than the unperturbed radii R_g of each sample.

Theoretical treatments^{24,25} show that in the weak overlap regime, assuming no interaction between the buoy block and the surface, the ratio of the thickness $2\Gamma_1/\Gamma_0$ to the radius of gyration is approximately $H_{\text{elli}}/R_g = 2.2$, which is in good agreement with the observed data. This observation confirms that the PS/PVP copolymers are generally tethered through the PVP block, with only very weak interactions between the PS buoy blocks and the surface.

Above $\Gamma/\Gamma^0 \approx 2$ the thickness begins to grow with increasing surface coverage, approaching a $(\Gamma/\Gamma^0)^{1/3}$ power-law at the highest overlap densities in the two largest and most asymmetric samples. The one-third power law is expected for neutral polymer brushes swollen in a good solvent environment.^{26,27} The data, nevertheless, indicate a gradual rather than a sharp transition to the one-third power-law regime, consistent with recent simulation²⁸ and mean-field results.²⁹ An attempt to quantify the experimental power law, however, would be imprecise due to the narrow range of overlap densities covered in the adsorption process. Nonetheless, the 225K/24K and 100K/12K samples are able to stretch up to 36% after 8 h of adsorption. The two smaller samples stretch slightly less, only achieving about 25% extension in their thickness.

The data indicate that the adsorbed copolymer layer is able to rearrange more quickly than the rate at which free chains adsorb to the surface. No matter how a chain arrives to the surface, the layer quickly tends toward its equilibrium thickness, growing at a rate that approaches the $(\Gamma/\Gamma^0)^{1/3}$ power law. This suggests that an adsorbing chain is reconfiguring quickly enough such that the PS buoy block extends from the surface anchored through the insoluble PVP block. On the other hand, if a significant attraction existed between the PS block and the surface, the adsorbed layer perhaps would get trapped in long-lived transitional states where the thickness increase would resemble homopolymer adsorption rather than diblock copolymer adsorption from a selective solvent. The layer structure at each stage in the adsorption process is important as it dictates the potential barrier that a free chain must overcome to adsorb; therefore, the overall adsorption kinetics is governed by the exact structure of the adsorbed layer. Assuming that the thickness of the adsorbing layer

grows as $(\Gamma/\Gamma^0)^{1/3}$ and is independent of the adsorption rate, Johner and Joanny theoretically showed that the adsorbed amount should increase as $(\log t)^{6/5}$ at long times.¹² In practice, however, a true test of this scaling law is difficult as not enough decades of time can be practically collected to precisely verify the 6/5 dependence. For instance, it takes approximately 1 h for the 100K/12K sample to reach 3 mg/m². To double this adsorbed amount would take another 1 year if the rate followed $(\log t)^{6/5}$ kinetics. Nonetheless, the present data set strongly suggests that PS/PVP adsorption from toluene would be well described by the $(\log t)^{6/5}$ power law as the thickness of the layer at sufficiently long times is well described by the $(\Gamma/\Gamma^0)^{1/3}$ power law.

Conclusions

It was demonstrated that ellipsometry can be used to monitor in situ and simultaneously both the thickness and the adsorbed amount of a series of PS/PVP diblock copolymers adsorbed from a selective solvent to help clarify structure evolution and molecular rearrangements during the adsorption process. Such information ultimately leads to a more thorough understanding of the interplay between kinetic and thermodynamic issues in governing the adsorbed layer structure. We used a diblock copolymer with a soluble polystyrene block that shows very little interaction with the surface. Indeed without the poly(2-vinylpyridine) block, polystyrene does not adsorb. Therefore, it may be expected that any molecular rearrangements may be fast as few polystyrene-surface contacts have to be broken or displaced. If instead polystyrene could directly adsorb to the surface, then these rearrangements would be much more sluggish and the so-called "brush" structure would not clearly emerge on practical time scales.

Acknowledgment. Helpful discussions are acknowledged with David Beaglehole, John Lekner, S. Michael Kilbey, II., and Roger Pynn. This work was supported by the NIRT Program and MRL Program of the National Science Foundation under Awards CTS-0103516 and DMR-0080034.

Appendix: Ellipsometry Analysis of Highly Solvated, Adsorbed Polymer Layers

The ellipsometric analysis of thin, solvated films offers a challenge for two reasons. First, the refractive index of the adsorbed layer approaches that of the surrounding medium, providing very poor optical contrast. Second, a functional form of the density profile must be assumed in order to resolve the overall thickness. Historically, the common approach is to assume the density through the layer is a constant and to analyze the film as a step profile.³⁰ Based on this one-layer model, both an average refractive index n_{av} and average thickness h_{av} can be calculated for the adsorbed layer. However, these values yield the properties of a homogeneous film that give rises to the same ellipsometric ratio as the actual profile. The relationship between h_{av} and the actual thickness can be ambiguous.

In the limit where the reflection from the adsorbed layer only slightly deviates from the reflection between the solvent and the substrate, the layer can be analyzed with respect to the ideal Fresnel interface plus correction terms.²¹

$$\rho = \frac{r_{p0}}{r_{s0}} + \frac{r_{p1}}{r_{s1}} + \frac{r_{p2}}{r_{s2}} + \dots \quad (\text{A.1})$$

where r_{p0} and r_{s0} refers to the reflection coefficients between the solvent and the substrate and the terms with subscripts 1 and 2 refer to the first- and second-order corrections. These corrections are expressed in terms of integral invariants J_{ij} , which describe the difference between the actual dielectric profile and the dielectric profile taken for the Fresnel interface:

$$\frac{r_{p1}}{r_{p1}} = -\frac{2i}{r_{s0}} \frac{Q_1}{(Q_1 + Q_2)^2} \frac{K^2}{\epsilon_1 \epsilon_2} J_1 \quad (\text{A.2})$$

$$\frac{r_{p2}}{r_{p2}} = \frac{2Q_1 K^2}{r_{s0}(Q_1 + Q_2)^2} \left[\frac{(K^2/\epsilon_1^2 \epsilon_2^2)}{Q_1 + Q_2} J_1^2 + \frac{Q_2 J_{2,2} - (1/\epsilon_1 + 1/\epsilon_2) J_{2,1}}{\epsilon_1 - \epsilon_2} \right] \quad (\text{A.3})$$

where ϵ_i are the dielectric constants ($\epsilon_i = n_i^2$), K is the tangential component of the wave vector

$$K = \left(\frac{2\pi}{\lambda} \right) n_i \sin \varphi_i \quad (\text{A.4})$$

and Q_i is the normal component of the wave vector in medium i :

$$Q_i = \left(\frac{2\pi}{\lambda} \right) \frac{\cos \varphi_i}{n_i} \quad (\text{A.5})$$

Terms with the subscript 2 refer to the transmitted medium (the substrate) and terms with the subscript 1 refer to the incident medium. At the Brewster angle θ_B for the solvent/substrate interface, eqs 2–4 can be vastly simplified. The Brewster angle is defined as the condition where $\theta_B = \arctan(n_2/n_1)$. If neither the solvent nor the substrate have an imaginary component to their refractive index, the following relationships are true at the Brewster angle:

$$r_{p0} = 0 \quad (\text{A.6})$$

$$r_{s0} = \frac{\epsilon_2}{\sqrt{\epsilon_1 + \epsilon_2}} \quad (\text{A.7})$$

$$Q_1 = Q_2 = \frac{K}{\sqrt{\epsilon_1 \epsilon_2}} = \frac{2\pi}{\lambda} \frac{1}{\sqrt{\epsilon_1 + \epsilon_2}} \quad (\text{A.8})$$

With these simplifications, eq A.3 becomes

$$\rho = i\pi \frac{\sqrt{\epsilon_1 + \epsilon_2}}{\epsilon_1 - \epsilon_2} \left(\frac{J_1}{\lambda} \right) + \frac{\pi^2}{\epsilon_1 - \epsilon_2} \left[\left(\frac{J_1}{\lambda} \right)^2 + 2 \frac{\epsilon_1 \epsilon_2}{\epsilon_1 - \epsilon_2} \left(\frac{J_{2,1}}{\lambda^2} \right) - 2 \frac{\epsilon_1 + \epsilon_2}{\epsilon_1 - \epsilon_2} \left(\frac{J_{2,2}}{\lambda^2} \right) + \dots \right] \quad (\text{A.9})$$

The full forms of the invariants are listed in a publication by J. Lekner.²¹ For small perturbations in the dielectric constant, the three invariants can be expanded to first order in $\Delta\epsilon$, which is the difference between the dielectric of the adsorbed layer and the pure solvent

$$J_1 = \frac{\epsilon_1 - \epsilon_2}{\epsilon_2} \Gamma_0^\epsilon + O[(\Delta\epsilon)^2] \quad (\text{A.10})$$

where Γ_i^ϵ is the i th moment associated with the dielec-

$$J_{2,1} = 2(\epsilon_1 - \epsilon_2) \Gamma_1^\epsilon + O[(\Delta\epsilon)^2] \quad (\text{A.11})$$

$$J_{2,2} = \frac{4(\epsilon_1 - \epsilon_2)}{\epsilon_2} \Gamma_1^\epsilon + O[(\Delta\epsilon)^2] \quad (\text{A.12})$$

tric profile:

$$\Gamma_i^\epsilon(\Delta\epsilon) = \int_0^\infty \Delta\epsilon(z) z^i dz \quad (\text{A.13})$$

A further simplification that can be made is

$$\Delta\epsilon(z) \approx 2n_2 \Delta n(z) \quad (\text{A.14})$$

Substitution of eqs A.10–A.13 in eq A.9 finally yields a simple analytical relationship between the ellipsometric ratio ρ and the moments Γ_1 and Γ_0 of the refractive index profile at the Brewster angle for the substrate/solvent interface:

$$\rho = i(2\pi) \frac{\sqrt{n_1^2 + n_2^2}}{n_2} \left(\frac{\Gamma_0}{\lambda} \right) + (2\pi)^2 n_2 \left(\frac{2\Gamma_1}{\lambda^2} \right) \quad (\text{A.15})$$

where

$$\Gamma_i(\Delta n) = \int_0^\infty \Delta n(z) z^i dz \quad (\text{A.16})$$

This relationship shows that the imaginary part of the ellipsometric ratio ($\text{Im}(\rho) = \tan \Psi \cos \Delta$) is proportional to the zeroth moment of the index profile and the real part of the ratio ($\text{Re}(\rho) = \tan \Psi \sin \Delta$) is proportional to the first moment of the index profile. In the absence of any layer $\rho = 0$.

References and Notes

- Halperin, A.; Tirrell, M.; Lodge, T. *Adv. Polym. Sci.* **1992**, *100*, 31–71.
- Marques, C.; Joanny, J. F.; Leibler, L. *Macromolecules* **1988**, *21*, 1051–1059.
- Johner, A.; Joanny, J. F.; Marques, C. *Physica A* **1991**, *172*, 285–289.
- Satija, S. K.; Majkrzak, C. F.; Russell, T. P.; Sinha, S. K.; Sirota, E. B.; Hughes, G. J. *Macromolecules* **1990**, *23*, 3860–3864.
- Field, J. B.; Toprakcioglu, C.; Ball, R. C.; Stanley, H. B.; Dai, L.; Barford, W.; Penfold, J.; Smith, G.; Hamilton, W. *Macromolecules* **1992**, *25*, 434–439.
- Field, J. B.; Toprakcioglu, C.; Dai, L.; Hadzioannou, G.; Smith, G.; Hamilton, W. *J. Phys. II* **1992**, *2*, 2221–2235.
- Cosgrove, T.; Phipps, J. S.; Richardson, R. M.; Hair, M. L.; Guzonas, D. A. *Macromolecules* **1993**, *26*, 4363–4367.
- Hadzioannou, G.; Patel, S.; Granick, S.; Tirrell, M. *J. Am. Chem. Soc.* **1986**, *108*, 2869–2876.
- Parsonage, E.; Tirrell, M.; Watanabe, H.; Nuzzo, R. G. *Macromolecules* **1991**, *24*, 1987–1995.
- Tirrell, M.; Parsonage, E.; Watanabe, H.; Dhoot, S. *Polym. J.* **1991**, *23*, 641–649.
- Belder, G. F.; ten Brinke, G.; Hadzioannou, G. *Langmuir* **1997**, *13*, 4102–4105.
- Johner, A.; Joanny, J. F. *Macromolecules* **1990**, *23*, 5299–5311.
- Tassin, J. F.; Siemens, R. L.; Tang, W. T.; Hadzioannou, G.; Swalen, J. D.; Smith, B. A. *J. Phys. Chem.* **1989**, *93*, 2106–2111.
- Munch, M. R.; Gast, A. P. *J. Chem. Soc., Faraday Trans.* **1990**, *86*, 1341–1348.

- (15) Munch, M. R.; Gast, A. P. *Macromolecules* **1990**, *23*, 2313–2320.
- (16) Motschmann, H.; Stamm, M.; Toprakcioglu, C. *Macromolecules* **1991**, *24*, 3681–3688.
- (17) Amiel, C.; Sikka, M.; Schneider, J. W.; Tsao, Y. H.; Tirrell, M.; Mays, J. W. *Macromolecules* **1995**, *28*, 3125–3134.
- (18) Pelletier, E.; Stamouli, A.; Belder, G. F.; Hadziioannou, G. *Langmuir* **1997**, *13*, 1884–1886.
- (19) Azzam, R. M.; Bashara, N. M. *Ellipsometry and Polarized Light*; North-Holland Publication: Amsterdam, 1979.
- (20) Charmet, J. C.; deGennes, P. G. *J. Opt. Soc. Am.* **1983**, *73*, 1777–1784.
- (21) Lekner, J. *Physica* **1984**, *128A*, 229–252.
- (22) Jaspersion S.; Schnatterly S. *Rev. Sci. Instrum.* **1969**, *40*, 761–&.
- (23) Higo, Y.; Ueno, N.; Noda, I. *Polym. J.* **1983**, *5*, 367–375.
- (24) Carignano, M. A.; Szleifer, I. *Macromolecules* **1995**, *28*, 3197–3204.
- (25) Weinhold, J. D.; Kumar, S. K.; Szleifer, I. *Europhys. Lett.* **1996**, *35*, 695–700.
- (26) de Gennes, P. *Macromolecules* **1980**, *13*, 1969–1075.
- (27) Milner, S.; Witten, T.; Cates, M. *Macromolecules* **1988**, *21*, 2610–2619.
- (28) Pepin, M. P.; Whitmore, M. D. *J. Chem. Phys.* **1999**, *111*, 10381–10388.
- (29) Baranowski, R.; Whitmore, M. D. *J. Chem. Phys.* **1995**, *103*, 2343–2353.
- (30) de Feijter, J. A.; Benjamins, J.; Veer, F. A. *Biopolymers* **1978**, *17*, 1759–1772.

MA034974Y